Supporting Information

Payload drug *vs.* Nanocarrier Biodegradation by Myeloperoxidase- and Peroxynitrite-Mediated Oxidations: Pharmacokinetic Implications

Wanji Seo,[a] Alexandr A. Kapralov,[b] Galina V. Shurin,[c] Michael R. Shurin,[c,d] Valerian E. Kagan[b], Alexander Star*[a]

a. Department of Chemistry, University of Pittsburgh, Pittsburgh, PA 15260, USA

b. Department of Environmental and Occupational Health, University of Pittsburgh, 100 Technology Drive, Pittsburgh, PA 15219, USA

c. Department of Pathology, University of Pittsburgh Medical Center, Pittsburgh, PA 15261, USA

d. Department of Immunology, University of Pittsburgh Medical Center, Pittsburgh, PA 15261, USA

Correspondence email: astar@pitt.edu

Table of contents

1. General information

Materials

HiPco SWCNT was purchased from NanoIntegris®. Lyophilized human myeloperoxidase (MPO) was received from Athens Research and Technology, INC. (Athens, GA, USA). N-(aminopropylpolyethyleneglycol)carbamyl-disteaoyl phosphatidylethanolamine (DSPE-050PA) was purchased from NOF Corporation. (Methyl-PEG_{12})$_3$-PEG-NHS Ester (TMS$(PEG)_{12}$) was obtained from Thermo Scientific. N_3-(2-Hydroxy-2-nitroso-1-propylhydrazino)-1-propanamine (Papa NONOate) was purchased from Cayman Chemical Company (Ann Arbor, MI). All other chemicals were purchased from Sigma Aldrich, and were used without further purification. All samples were prepared by dispersing dry solid in either nanopure water or phosphate buffer (pH 7.4).

Instrumental

Nanopure water was collected from Thermo Scientific Barnstead^{TM} Nanopure^{TM}. Branson 5510 was used for ultrasonication. Thermo Scientific Savant SPD 1010 SpeedVac was employed to dry aqueous samples (pressure: 5.6 Torr, temperature: 45 ˚C). The size distribution and the morphology were analyzed with Transmission Electron Microscopy (FEI-Morgani, 80 keV). All UV-Vis-NIR spectra were acquired using a Lambda 900 spectrophotometer (PerkinElmer). Fluorescent spectra were taken using a Horiba Jovin Yobin Fluoromax 3. Renishaw inVia Raman microscope was utilized to collect Raman spectra (laser $\lambda_{excitation}$: 633 nm). Fourier Transform spectroscopy (FTIR) was performed employing an IR-Prestige spectrophotometer (Shimadzu Scientific) outfitted with an EasiDiff accessory (Pike Technologies). X-ray photoelectron

spectroscopy (XPS) was obtained via a Thermo Scientific ESCALAB 250xi photoelectron spectrometer using monochromated Al K Alpha X-rays as the source. A reverse-phase LC/MS (LC/MS-2020 Shimadzu) equipped with a Phenomenex C18 column and a photodiode array (PDA) detector was utilized. MALDI mass spectra were recorded on a MALDI, Voyager-DE PRO Instrument. Zeta potential was measured using a Brookhaven ZetaPals at 25 ˚C under specified conditions of pH. NMR spectra were acquired on a Bruker Avance III 400MHz NMR. Chemical shifts were reported in ppm (δ) relative to residual solvent peaks (DMSO-d_6 = 2.50 ppm for ^{1}H). Coupling constants (*J*) were reported in Hz. C18 column chromatography was performed on a C_{18}-reversed phase silica gel purchased from Sigma-Aldrich.

2. Synthesis of materials

Raw HiPco (NanoIntegris®) single-walled carbon nanotubes (25 mg) were oxidized in 50 mL of an acid mixture (H_2SO_4 /HNO_3, 3/1, v/v) in an ultrasonic bath set at 25 ˚C over 3 h 20 min. After thorough washing with distilled water several times, the oxidized nanotubes were dried under vacuum over 24 h, which yielded 18 mg of OX-SWCNTs. A phospholipid functionalized PEG (PL-PEG) was prepared by an amide coupling with DSPE-050PA (115 mg) and TMS$(PEG)_{12}$ (71 mg) in anhydrous dichloromethane (3.0 mL). After 12 h, in the case when much of the reactants still remained due to mostly the hydrolyzed –N-hydroxysuccinimide (NHS) group of TMS$(PEG)_{12}$, N,N-Dicyclohexylcarbodiimide (DMAP) (20 mg) and 4-dimethylaminopyridine (10 mg) were added, and amide formation proceeded . After 24 h of stirring at room temperature, the solvent was dried, and the reaction mixture was washed with nanopure water (61 mL) and was collected through vacuum filtration. Excess DMAP was further removed through dialysis. This reaction gave an average MW of ca. 7.4–8.2 kDa of PL-PEG (Fig. S1).

The ox-SWCNTs were sonicated with PL-PEG in phosphate buffer (pH 8.2) for 1 h and then stirred at room temperature. The PEGylated ox-SWCNT was washed low molecular weight PEG chains with ultracentrifugation (11,000 rpm, 30 min × 3) using a 100 kDa Amicon centrifugal filter. Doxorubicin (4.8 mg) was dissolved in 10 mL of phosphate buffer (0.1 M, pH 8.2). The DOX solution was sonicated for 30 min and was stirred overnight. After thorough washing with the same buffer solution through centrifugation, the amount of DOX wash-off was calculated from a UV-Vis calibration curve. The reaction gave about 2.3 mg of DOX bound to 3.0 mg of ox-SWCNT/PL-PEG, which gave a 77% of drug loading. This estimation differs by 23% from the UV-Vis titration (Fig. S6).

3. Characterization of phospholipid-polyethylene glycol (PL-PEG)

MALDI mass spectrometry A matrix solution was prepared with α-Cyano-4-hydroxycinnamic acid (10.0 mg) in a 2 mL mixture of equal volumes of 0.2 % of trifluoroacetic acid (TFA) in H_2O and CH_3CN. A PL-PEG was dispersed in water (1 mg/mL) and then mixed with the prepared CH_3CN/TFA solution (1:1, v/v).

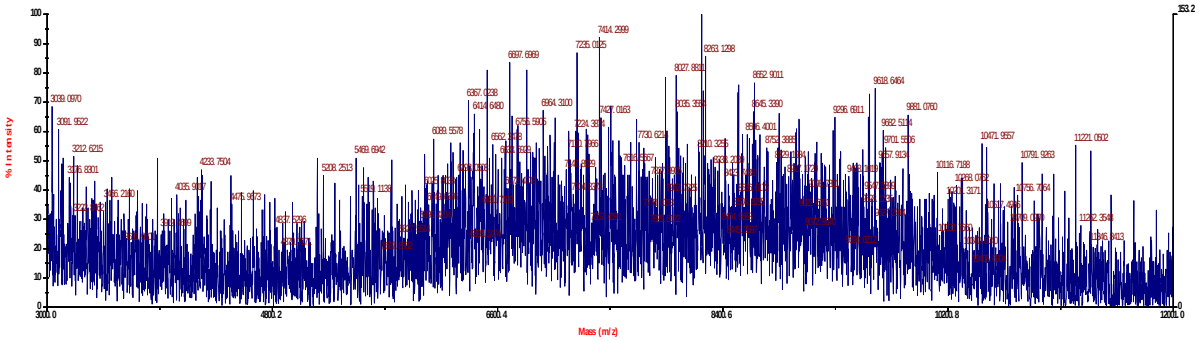

Fig. S1 MALDI mass spectrum of PL-PEG. The average molecular weight was estimated around 7.4– 8.2 KDa.

4. Characterization of oxidized HiPco SWCNTs (ox-SWCNT)

Raman spectroscopy Dried nanotubes were drop-cast on a microscope slide. Spectra were collected with a 10 second exposure time and averaged across 5 scans per location. The collected spectra were normalized to 1 with respect to the maximum intensity. After 3 h 20 min of an acid treatment (H_2SO_4: HNO_3, 3:1, v/v) with ultrasonication, the D band became wider and was shifted to a higher wavenumber. I_D/I_G of the ox-SWCNT was substantially larger than that of the pristine SWCNT, indicating the higher degree of functionalization.

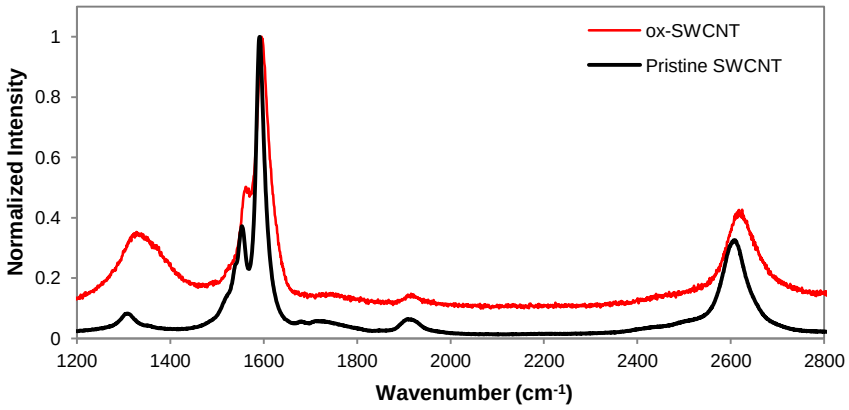

Fig. S2 Raman spectroscopy of pristine HiPco SWCNT and ox-SWCNT.

Nanotubes	D band (cm^{-1})	G band (cm^{-1})	I_D/I_G intensity ratio
Pristine SWCNT	1309	1591	0.08
ox-SWCNT	1327	1596	0.35

Fourier transform spectroscopy (FTIR) ox-SWCNTs were homogeneously mixed with KBr. Using KBr as the background and taking 32 scans per sample, a spectrum was obtained over the range of 800 to 4000 cm^{-1} with a resolution of 4 cm^{-1}.

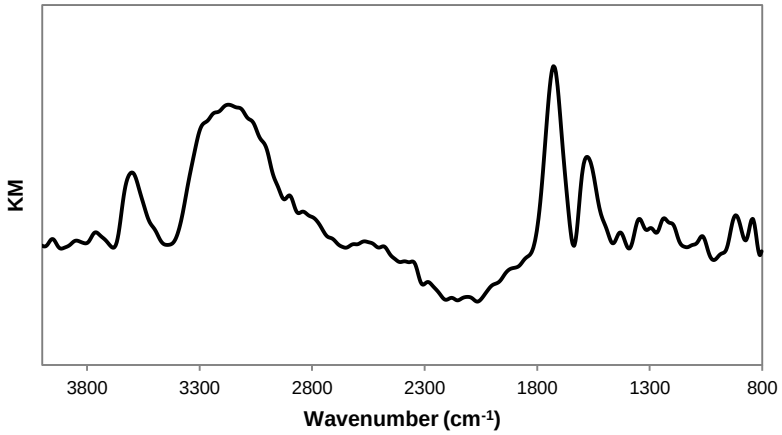

Fig. S3 Fourier transform infrared spectrum of ox-SWCNT.

Peak (cm^{-1})	Functional group
3587	Ar–**OH**
2684–3433	(C=O)–**OH**
1728	(**C=O**)–OH
1567	–**C=C**–
1334	–**S=O**–

X-ray photoelectron spectroscopy (XPS) The spot size of the sample was 400 µm (microns) prepared on an aluminum plate. Charge compensation was provided by a low energy electron source and Ar^+ ions. Survey scans were collected using a pass energy of 150 eV, and high resolution scans were collected using a pass energy of 50 eV. The average percentage indicates a mean obtained by analyzing three different sample spots.

(a)

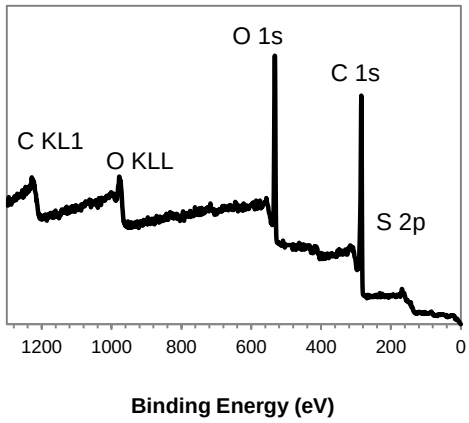

Element	Binding Energy (eV)	Relative Abundance (%)
C 1s	285.12	70.37
O 1s	532.47	25.22
S 2p	168.11	3.26

(b)

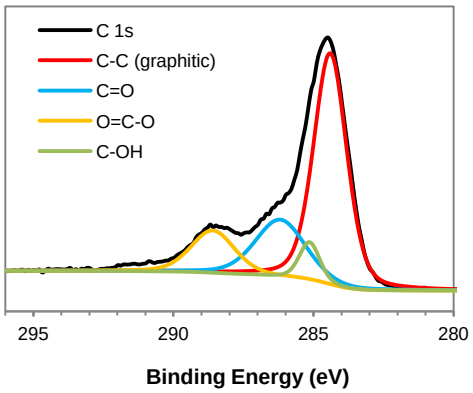

Surface functional group	Binding Energy (eV)	Relative Abundance (%)
C–C (graphitic)	284.40	58.50
C=O	286.19	21.64
O=C–O	288.59	14.04
C–OH	285.14	5.85

(c)

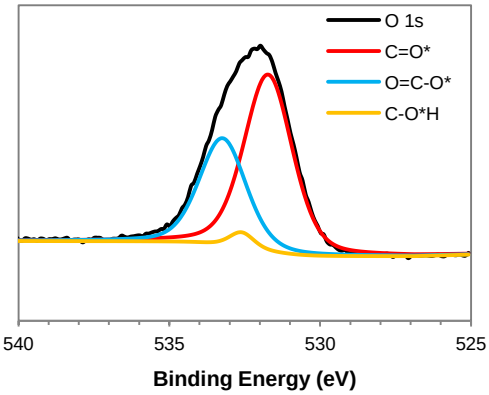

Surface functional group	Binding Energy (eV)	Relative Abundance (%)
O–C=O*	531.78	61.73
O=C–O*	533.23	35.80
C–O*H	532.64	2.47

Fig. S4 X-ray photoelectron spectroscopy (XPS) of ox-SWCNT. (a) Survey scan of the sample, (b) High resolution spectra of C 1s and fitting curves corresponding to different functional groups, and (c) High resolution spectra of O 1s and fitting curves.

5. Characterization of DOX-SWCNT

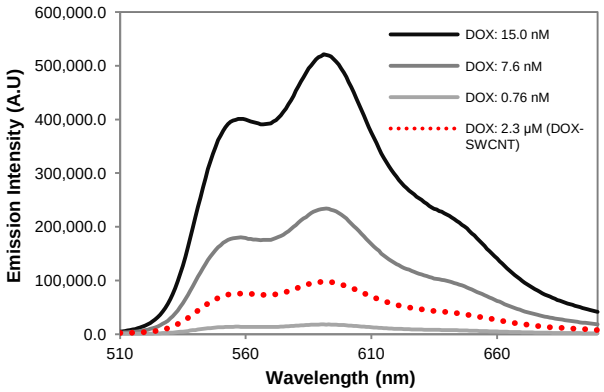

Fig. S5 Fluorescence emission spectra of DOX-SWCNT conjugate in comparison to free DOX of varying concentrations.

UV-Vis titration determining the binding ratio of ox-SWCNT/PL-PEG with DOX[S1] The maximum binding ratio of DOX to ox-SWCNT/PL-PEG was determined from the fitting curve. When the value of ΔA (ΔA = $A_{\text{bound DOX}} - A_{\text{freeDOX}}$) reaches the maximum, the binding of DOX to the nanotube is saturated, in which the wt equiv value (x) of the maximum is 0.964. Therefore, a 1:1 weight ratio of DOX to ox-SWCNT/PL-PEG was obtained from the fitting equation below.

$$y = y_0 + ae^{\left[-0.5\left(\left(\frac{ln\frac{x}{x_0}}{b}\right)^2\right)\right]} \quad (R^2 = 0.9870)$$

Fitting parameter	Coefficient	STD Error
a	0.0665	0.0049
b	0.3698	0.0382
x_o	1.0960	0.0386
y_o	0.0065	0.0026

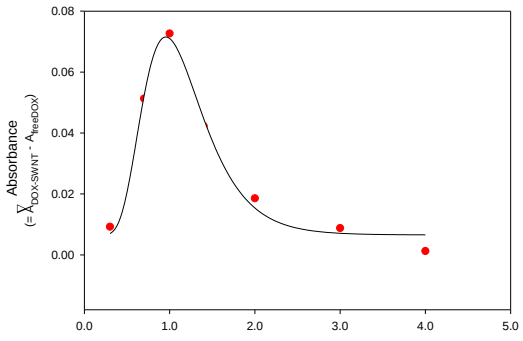

Fig. S6 UV-Vis titration of ox-SWCNT/PL-PEG with DOX. The fitting curve was found using SigmaPlot 11.0.

Zeta potential titration of ox-SWCNT/PL-PEG with DOX A solution of ox-SWCNT/PL-PEG in nanopure water (0.2 mg/mL) was prepared, and a 3 mL of the aliquot was transferred to a 20 mL scintillation vial. Then the varying amount of DOX solution in water (1.3 mg/mL) was added to the vial. After 30 min of sonication, the zeta potential of the solution mixture was measured with DLS. Using a graphical linear fitting curve near the saturation point at y-axis (0 mV), the corresponding wt equiv value was estimated. Approximately at 1.124 equiv, the zeta potential remains constant. Here, a 1.1:1 binding ratio of DOX to ox-SWCNT/PL-PEG was found. The graphical linear fit was obtained by OriginPro 8.5.

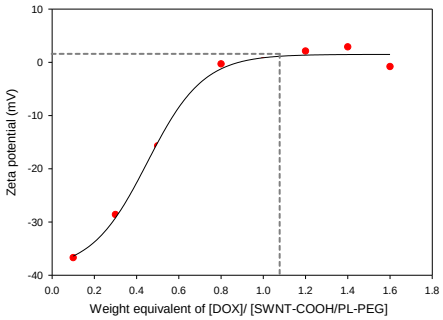

Fig. S7 Zeta potential titration of ox-SWCNT/PL-PEG with DOX.

6. Degradation experiments with myeloperoxidase, hydrogen peroxide, and chloride ($MPO/H_2O_2/Cl^-$)

Each DOX-SWCNT sample was prepared by dispersing 0.03 mg of DOX-SWCNT in 720 µL of phosphate buffer (pH 7.4, 0.1 M). The concentration of free DOX was 0.02 mg/mL. Stock solutions of DTPA and NaCl were added to the DOX-SWCNT solution, and their final concentrations were adjusted to 0.38 mM and 0.14 M respectively. The concentration of DOX-SWCNT was 0.04 mg/mL. For the experiment of $+MPO/+H_2O_2/+Cl^-$, 4.4 µg of MPO was added every 24 h, and the H_2O_2 stock solution (18.75 mM) was added every 4 h (total volume of 30 µL

per day). For −MPO/−H_2O_2/+Cl^-, the same amount of the pH 7.4 buffer solution was added. The samples were stored in a standard cell culture incubator at 37 ˚C. For UV-Vis-NIR analysis, samples were cooled at ambient temperature for about 10 min. Each spectrum was collected with 700 μL of a sample solution in a quartz sample holder (path length: 1 cm), and further absorbance was recorded after each new addition of H_2O_2. A 0.02 mg/mL of ox-SWCNT/PL-PEG solution was prepared in the same buffer condition. Then the same procedure was used to monitor the degradation of the nanocarrier.

7. Degradation under $MPO/H_2O_2/Cl^-$

Each of original sample was diluted 1:20 or 1:50 times with ethanol, and 3 μL of the diluted solution was placed on a lacey carbon copper grid and then permitted to dry in ambient conditions over 24 h.

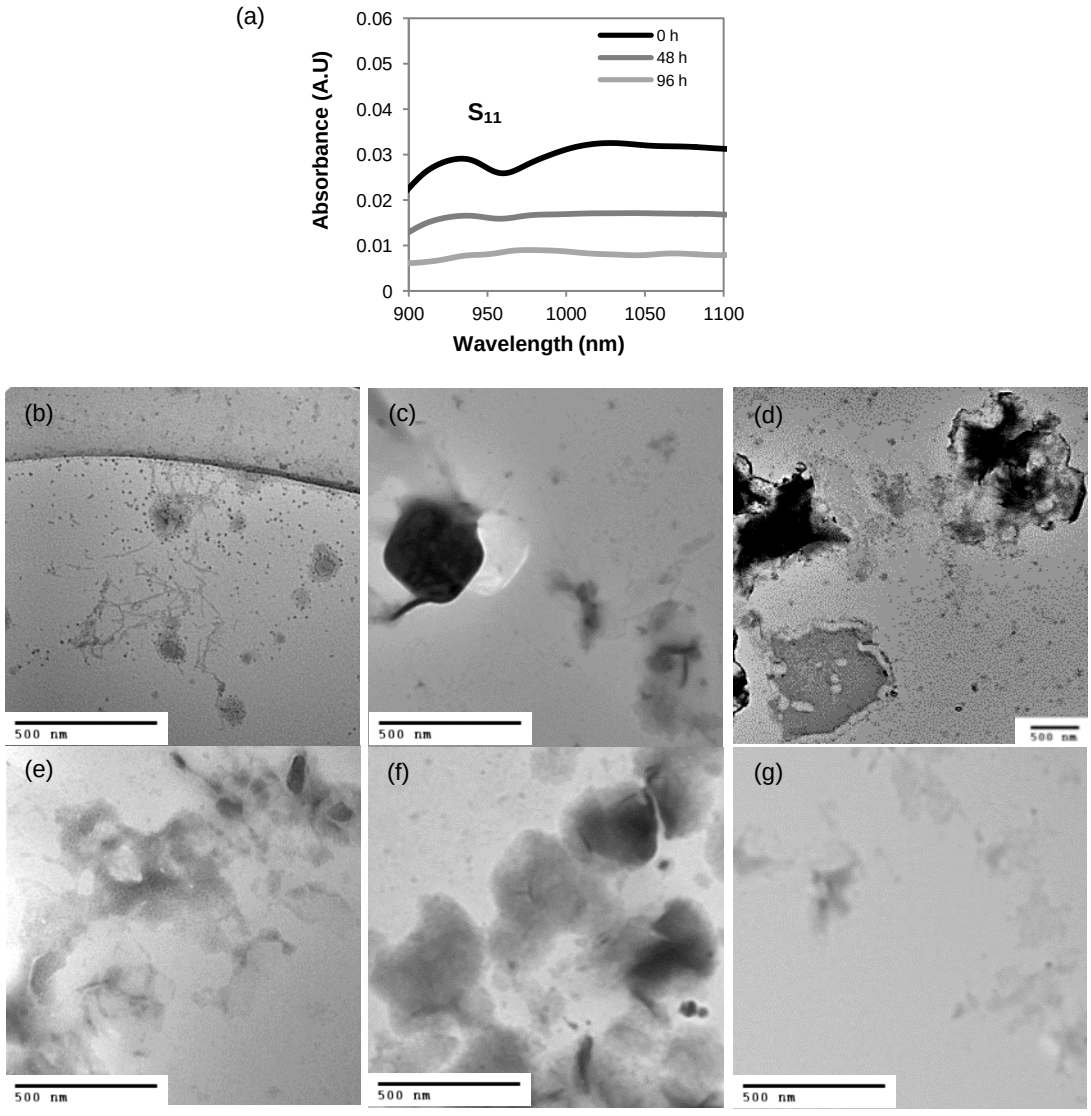

Fig. S8 (a) NIR spectral change in the S_{11} band of ox-SWCNT/PL-PEG and TEM images of degradation in phosphate buffer (0.1M, pH 7.4) of the same sample over (b) 0 h, (c) and (d) 24 h, (e) 48 h, (f) 72 h, and (g) 96 h.

8. Proposed degradation products of DOX formed under the conditions of +MPO/+H_2O_2/+Cl^- and −MPO/−H_2O_2/+Cl^- .

Scheme S1. (a) Degradation products of DOX possibly formed in the MPO-catalyzed oxidative and the control (non-oxidative) conditions (b) ox-SWCNT and its functional group transformations upon reaction with HOCl.

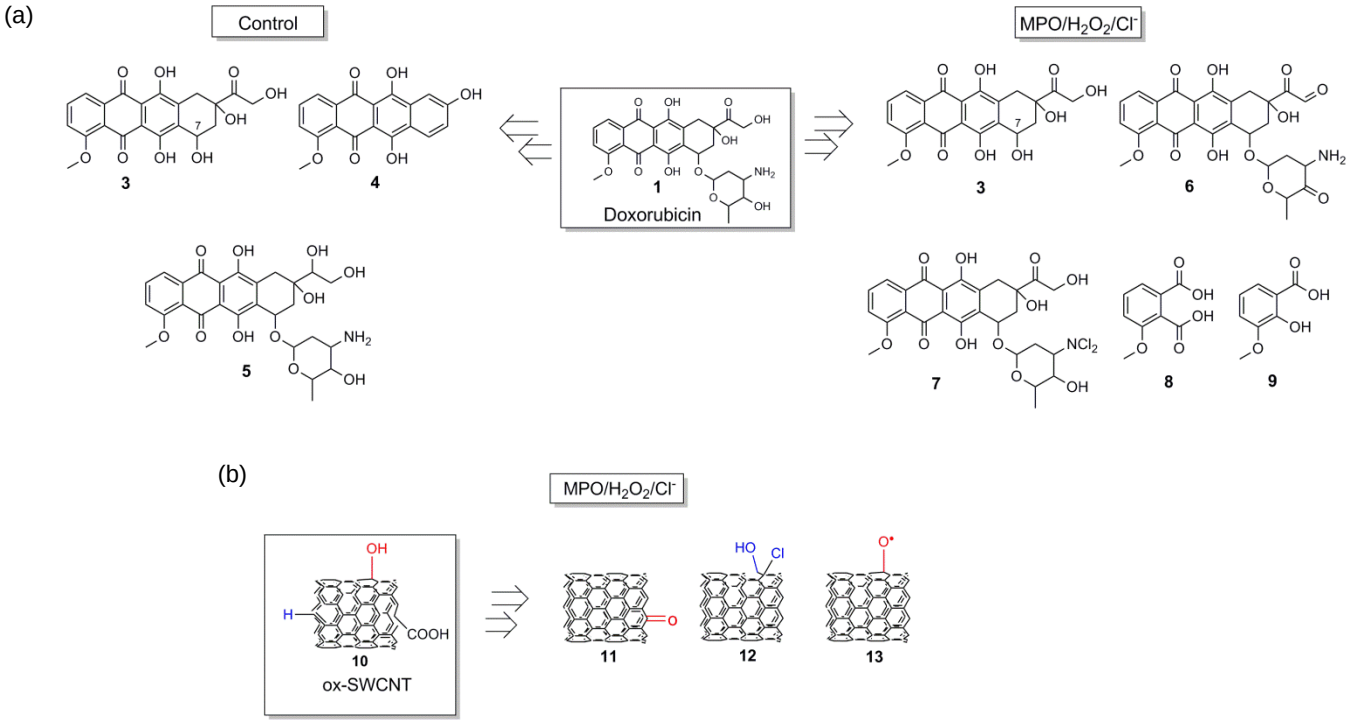

HOCl produced from MPO/H_2O_2/Cl^- can induce both oxidation and chlorination of DOX. The –OH groups undergo a transformation into the carbonyl groups of **6**,[S2] and the primary amine group are chlorinated selectively in **7**.[S3] Simultaneously, compound **11** can be formed from phenolic (–OH) groups of ox-SWCNTs. If the nanotubes contain dangling bonds terminated with –C=C– although this constituent is not abundant,[S4] compound **12** may provide another competing reaction with DOX.

Compounds **8** and **9** were previously identified in MPO/H_2O_2/NO_2^-, in which nitrite, a strong oxidant (or cofactor), promotes reduction of the hydroquinone moiety of the B-ring (Scheme 1).[S5] However, this pathway seems to less likely occur in our MPO/H_2O_2/Cl^- system.

Compound **3** is a known metabolite resulting from cleavage of the daunosamine by hydrolysis[S6] although its mechanism has not been well understood. However, **3** was not found in the control condition. In the case of *in vivo* experiments, we may see more different degradation pathways. Compounds **3** and **5** can be formed under reductive environments in cells. Cellular enzymes such as NADPH-cytochrome P450 reductase and flavoenzymes initiate transformation of the quinone of DOX to semiquinone (1e^- reduction) or hydroquinone (2e^- reduction).[S7] Compound **5** is formed by conversion of a ketone to an alcohol in ring A. Compound **3** is associated with various pathways, including electron transfer and quinone methide formation.[S8] No matter how the reduction process proceeds, DOX will eventually cleave the daunosamine, and a new bond is formed with nucleophiles, electrophiles, or radicals besides the hydroxyl group at C7 depending on the degradation pathway.

9. Identification of a degradation product (compound 4)

^{1}H NMR analysis In order to collect a large amount of sample for analysis, the weight and volume of each Doxorubicin solution was scaled up by 48 times while maintaining the same concentration used in the UV-Vis-NIR experiments. After incubation, the water in the samples was removed using SpeedVac over 6.5 h. The collected solid contained Doxorubicin degradation products and phosphate salt. Using methanol, N,N-dimethylformamide (DMF) and toluene, the collected samples were washed thoroughly and dried with a rotary evaporator and then a high vacuum pump over 24 h.

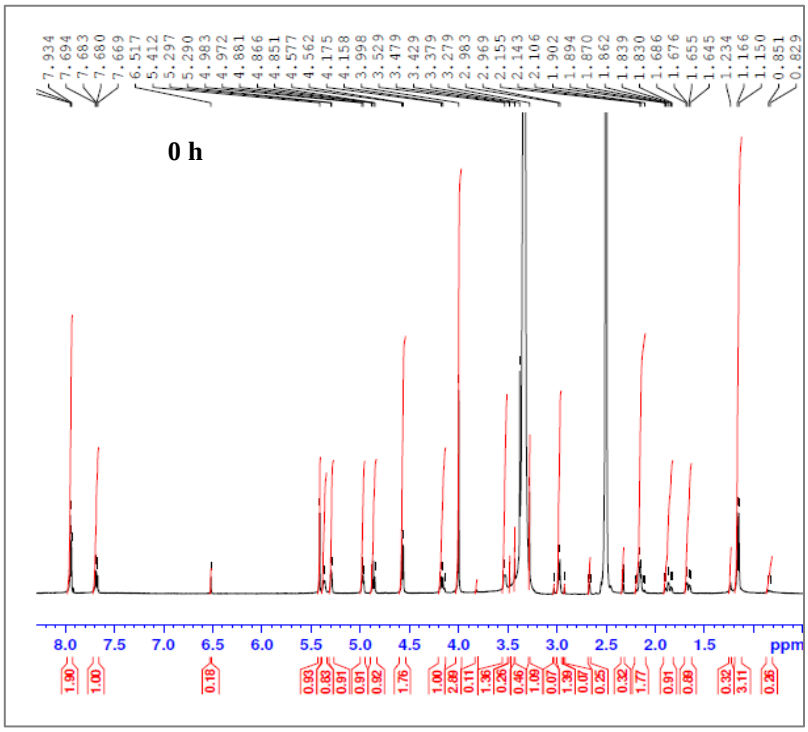

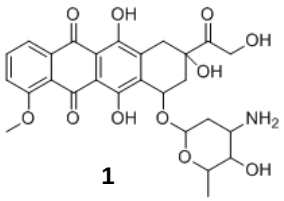

1

Fig. S9 ^{1}H NMR spectrum of free Doxorubicin (dimethyl sulfoxide-d_6, 400 MHz) at 0 h.

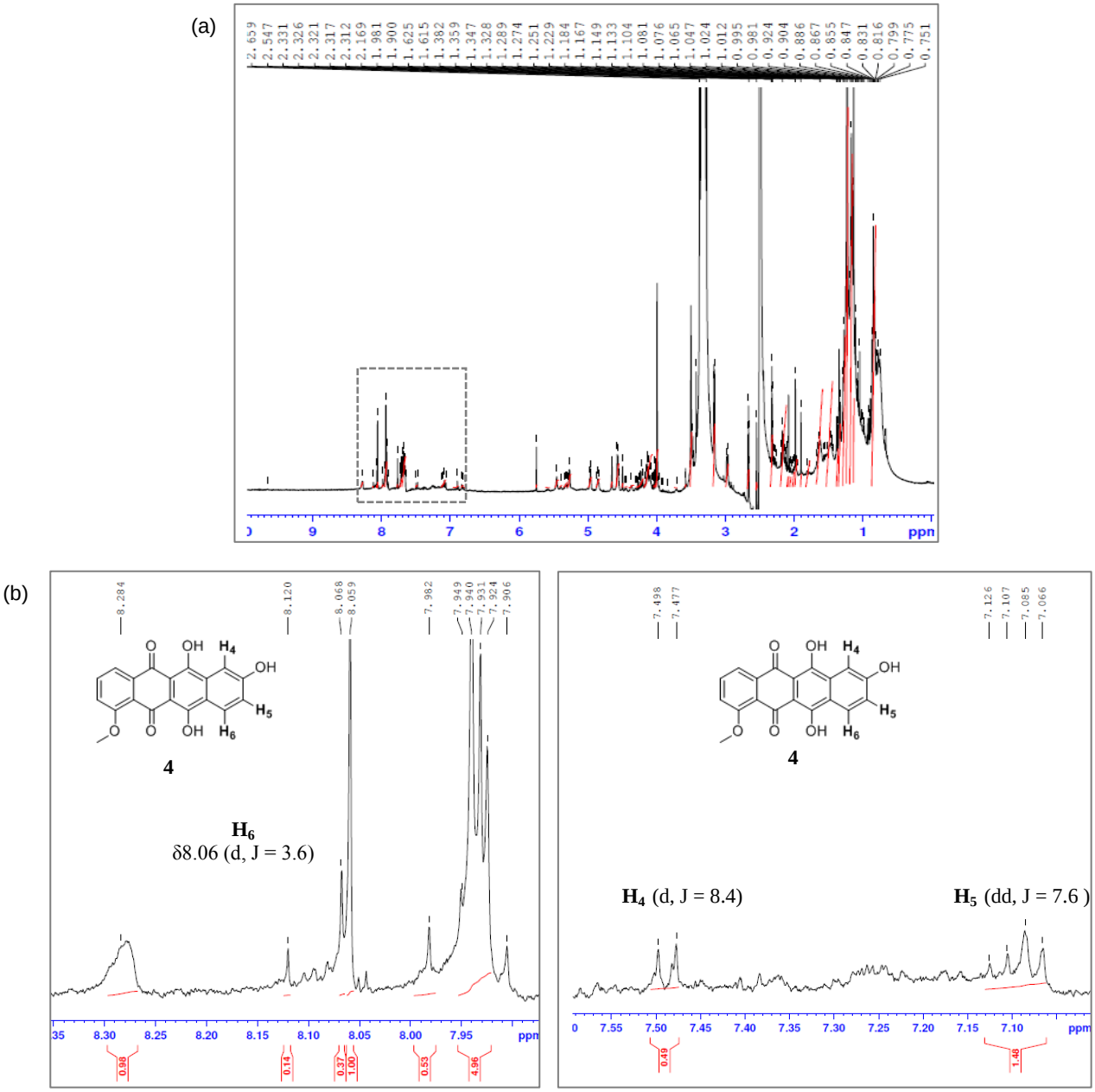

Fig. S10 (a) ^{1}H NMR spectrum of free DOX (−MPO/−H_2O_2) without purification after 32 h and (b) the aromatic proton shift region (δ7.0–8.3) of the same spectrum. The protons of compound **4** were assigned based on a precedent analysis[S9] and a predicted NMR data using Advanced Chemistry Development, INC. (ACS/Labs) Software V11.01 (©1994–2013 ACD/Labs).

LC/MS analysis Electro spray ionization (ESI-MS) was used to measure the mass of the degradation products. The samples were scanned in both positive and negative modes. H_2O and CH_3CN were used as eluents.

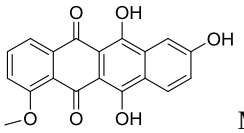

4

MW=336.30 g/mol

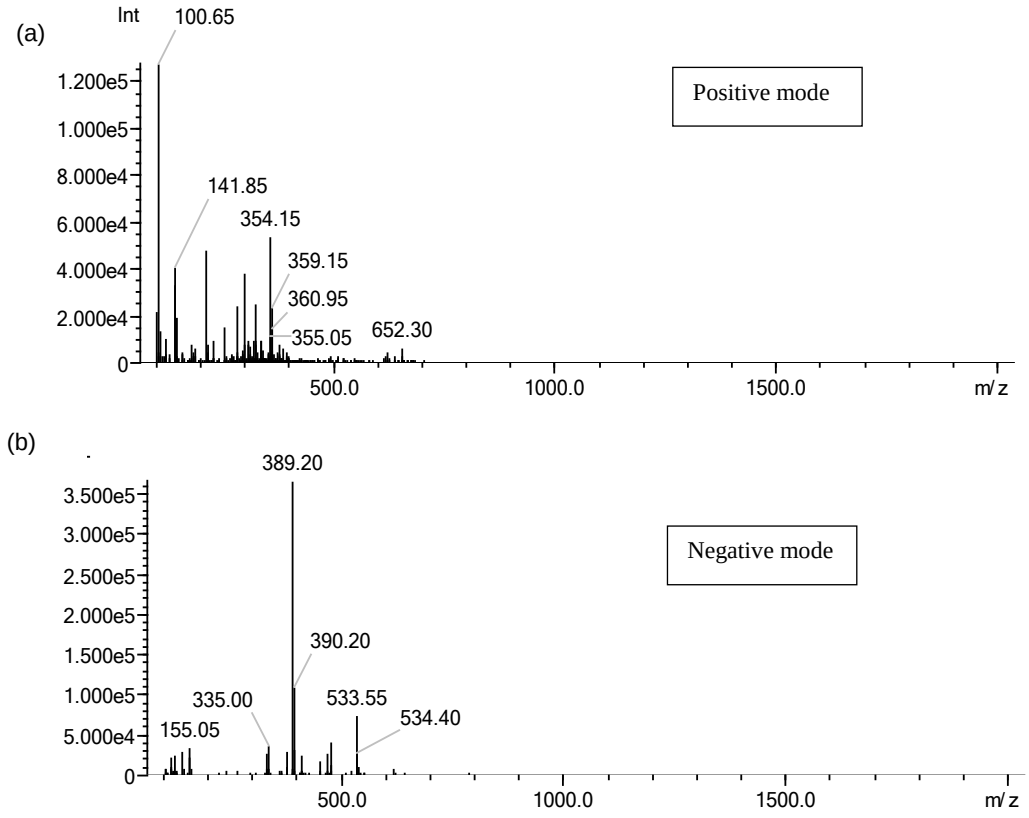

Fig. S11 LC/MS chromatograms and mass spectra of the control sample after 32 h. To remove the phosphate salt, these samples were purified with C18 mini-column chromatography. (a) The peak 359.15 (m/z) is an adduct of [MW + Na]. (b) The peak of 335 (m/z) is indicative of a negative adduct [MW−H].

10. Degradation experiments with peroxynitrite

Each DOX-SWCNT sample had a concentration of 0.03 mg of DOX-SWCNT in 808 μL of phosphate buffer (pH 7.4, 0.1 M), and 0.02 mg/mL of free DOX was prepared in the same buffer. Stock solutions of all other reagents were prepared every day. Then 7.5 μL of a xanthine oxidase (XO) solution (×50 diluted from the original enzyme) containing 0.15–0.3 mU of XO, was added per day, followed by additions of 7.5 μL of xanthine solution (7.0 mM) and 7.5 μL of a PAPA NONOate solution (3.5 mM) every 2 h (total 6 times per day). Due to the dilution effect, the concentrations of both xanthine and PAPA NONOate solutions were raised after 6 additions, maintaining the same amount of each reagent relative to the total volume of the DOX-SWCNT solution. After incubation over a given time period, all the samples were filtered using Amicon centrifuge filters (size: 1,000 Da). The filtrate and the concentrate were separately collected by ultracentrifuge (14,000 × g, 10 min), and the concentrate was further diluted in phosphate buffer (0.1M, pH 7.4) for proper analysis. Then fluorescence emission spectroscopy ($\lambda_{excitation}$: 488 nm, $\lambda_{emission}$: 592 nm) was utilized to measure the concentration of DOX-SWCNT within a linear calibration range at room temperature. Due to some loss of DOX-SWCNT after the ultracentrifugal filtration, a separate test determining the average recovery rate of DOX-SWCNT was performed to estimate the concentration accurately. The average recovery rate of five replicated samples was 62 ± 4 (%) from the original amount.

11. Characterization of peroxynitrite-mediated oxidation

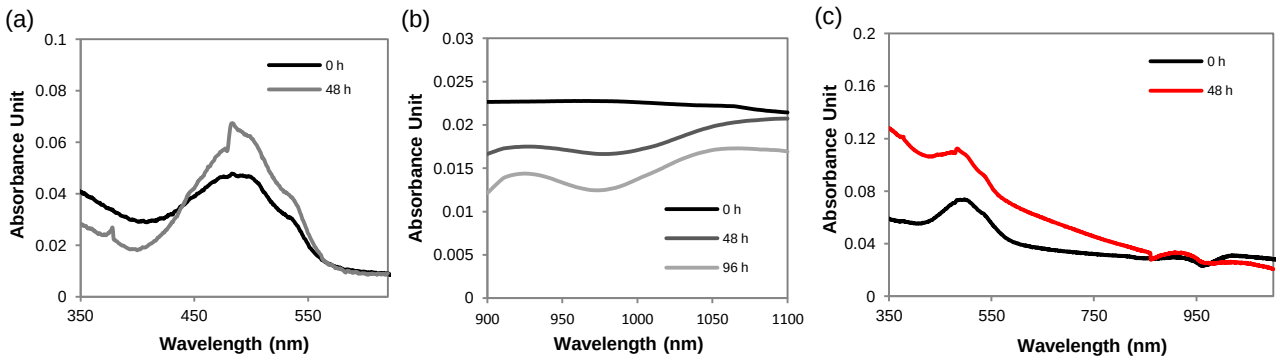

Fig. S12 (a) Degradation of free DOX after 48 h. Absorption increased at 480 nm probably due to the formation of a degradation product with the same absorption properties. (b) NIR absorption spectra of ox-SWCNT/PL-PEG and (c) UV-Vis-NIR absorption spectra of DOX-SWCNT (The spectra were normalized at 862 nm).

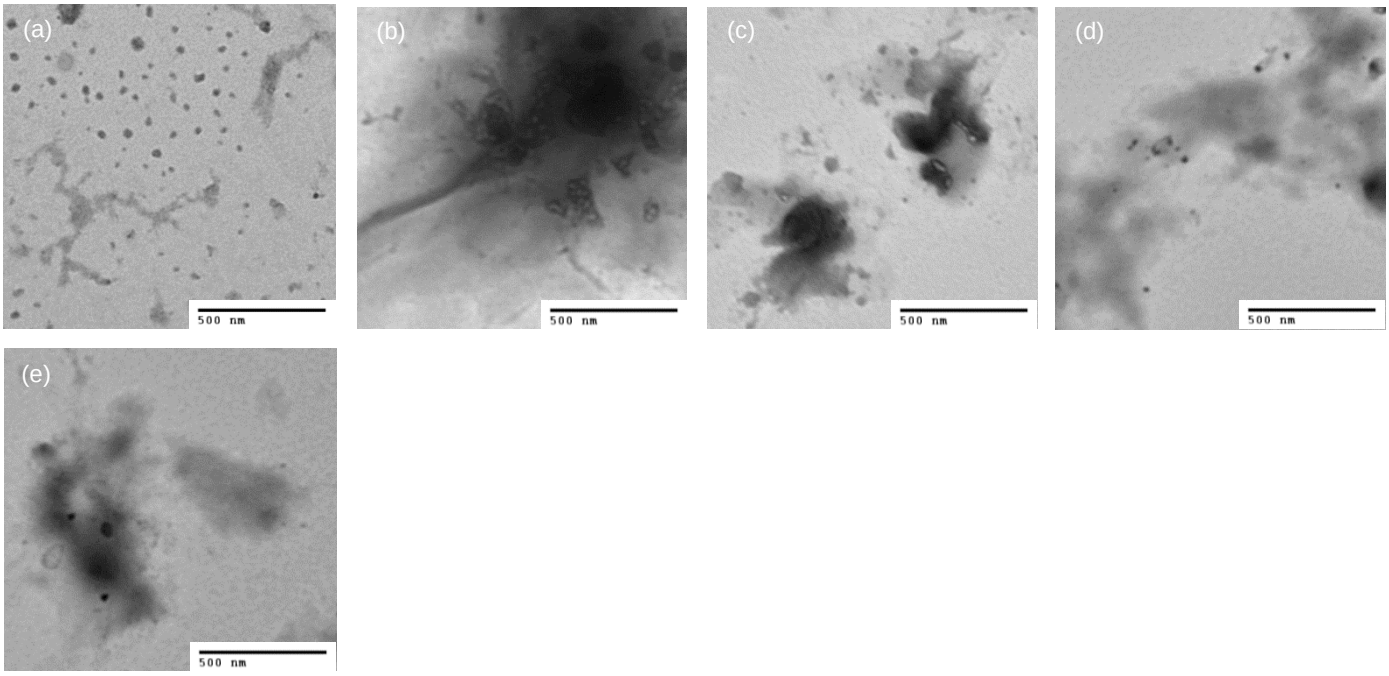

Fig. S13 TEM images of peroxynitrite-mediated degradation in phosphate buffer (0.1M, pH 7.4) of ox-SWCNT/PL-PEG over (a) 0 h, (b) 24 h, (c) 48 h, (d) 72 h, and (e) 96 h. TEM samples were prepared using the same method described in page S11.

12. Zeta potential titration with MPO

The laser of the zeta potential analyzer was set at 532 nm. The zeta potential of unbound pure MPO was measured separately, which gave a negative potential (−9.0 ± 1.7 mV). A rapid color change to a very bright yellow upon the laser irradiation suggests the photosensitive heme of MPO.[S10] After each titration, a sample containing DOX-SWCNT and MPO solutions was placed under ambient temperature and pressure over 1 h until their binding reached equilibrium, and then zeta potential was recorded. For the titration sample, solutions of DOX-SWCNT (0.3 mg/mL) and MPO were prepared in a mixture of nanopure water and 0.05 M, pH 7.4 phosphate buffer (17:1, v/v).

Table 1. Zeta potential changes upon sequential addition of each component of DOX-SWNT at pH 7.4.

Sample Name	Zeta Potential (mV)
SWNT-COOH	-48.3 ± 1.6
SWNT-COOH/PL-PEG	-34.3 ± 1.1
SWNT-COOH/PL-PEG/DOX	-14.2 ± 2.0
Free DOX	+9.2 ± 1.2

13. In vitro cell studies

Mice Pathogen-free C57BL/6 mice (7–8 wk old) mice from Jackson Labs (Bar Harbor, ME, USA) were individually housed and acclimated for 2 weeks. Animals were supplied with water and food *ad libitum* and housed under controlled light, temperature, and humidity conditions. All animal studies were conducted under a protocol approved by the Institutional Animal Care and Use Committee.

Cell B16 melanoma cells were obtained from American Type Culture Collection (ATCC, Manassas, VA, USA) and maintained in RPMI 1640 medium that was supplemented with 2 mM L-glutamine, 100 U/ml penicillin, 100 μg/ml streptomycin, 10 mM HEPES, 10% heat-inactivated FBS, 0.1 mM nonessential amino acids, and 1 mM sodium pyruvate (Invitrogen Life Technologies, Inc., Grand Island, NY, USA). Tumor conditioned medium was collected from sub-confluent cultures, centrifuged (300 g, 15 min) and cell-free supernatant was collected, aliquoted and used to treat MDSC.

For MDSC generation, bone marrow cells from tibia were isolated, filtered through a 70 μm cell strainer, and red blood cells were lysed with lysing buffer (155 mM NH_4Cl in 10 mM Tris-HCl buffer pH 7.5, 25°C) for 3 min. After RBC lysis, cells were washed and used for MDSC sorting. $CD11b^+$ $Gr\text{-}1^+$ MDSC were isolated from the bone marrow cell suspensions by magnetic cell sorting using a mouse MDSC Isolation Kit (MACS, Miltenyi Biotec, Auburn, CA, USA) according to the manufacturer's instructions. Isolated MDSC were cultured in supplemented RPMI 1640 medium with 25% (vol/vol) B16 conditioned medium for 48 h to generate tumor-activated MDSC expressing high levels of MPO.

Apoptosis assay CellTracker™ Orange CMTMR (5-(and-6)-(((4-chloromethyl)benzoyl)amino) tetramethylrhodamine) (Molecular Probes) was utilized to label B16 melanoma cell prior to co-culture experiments. The use of this fluorescent dye allowed distinguishing tumor cells and MDSC and assessing apoptosis in tumor cells. B16 cells and cells in mixed cultures were stained with Annexin V (Pharmingen) and the percentage of apoptotic Annexin V+ CMTMR+ cells was determined by flow cytometry (FacsCalibur, BD Biosciences, San Jose, CA, USA) and analyzed by FlowJo software.

Statistics Results were analyzed using one-way ANOVA and Student unpaired *t*-test with Welch's correction for unequal variances. All experiments were done in triplicates or repeated at least twice, and the results were presented as the means ± SEM (standard error of the mean). P values of < 0.05 were considered to be statistically significant.

Cell proliferation assay 3LL cells were labeled with CellTracker™ Orange CMTMR (5-(and-6)-(((4-chloromethyl)benzoyl)amino) tetramethylrhodamine) (Molecular Probes) and co-incubated with free DOX and DOX-SWCNT in the presence of tumor-activated MDSC. Co-incubation of 3LL cells with SWCNT, MDSC or both served as controls. After 24 h of incubation, the number of labeled 3LL cells was determined by flow cytometry (FacsCalibur) events calculated for 1 min. Increased number of cells (versus control medium group) suggests an increase in cell proliferation, while lower cell number reflects cytotoxic (cell death) and/or cytostatic (inhibition of cell proliferation) effects on tumor cells.

14. Concentrations of released DOX in cell medium

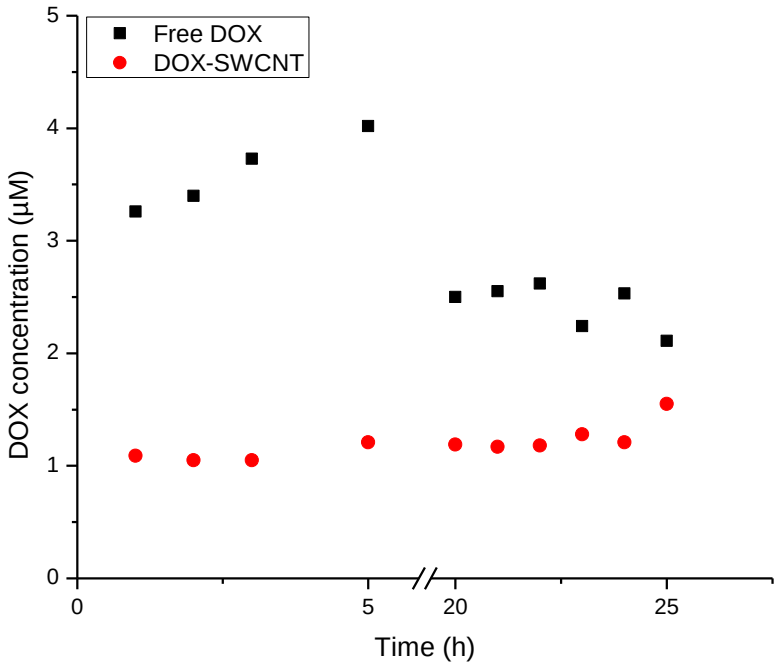

Fig. S14 MDSC were incubated in the medium containing 5 μM solutions of free DOX and DOX-SWCNT (with 100% drug loading). After 25 h, each supernatant of the drug-incubated cell medium was collected by centrifugation (10,000 g, 15 min), and the concentration of free DOX was estimated by measuring fluorescence emission intensity at 590 nm ($\lambda_{excitation}$=488 nm) using standard calibration fit.

15. Ex vivo pH-dependent DOX release from SWCNT

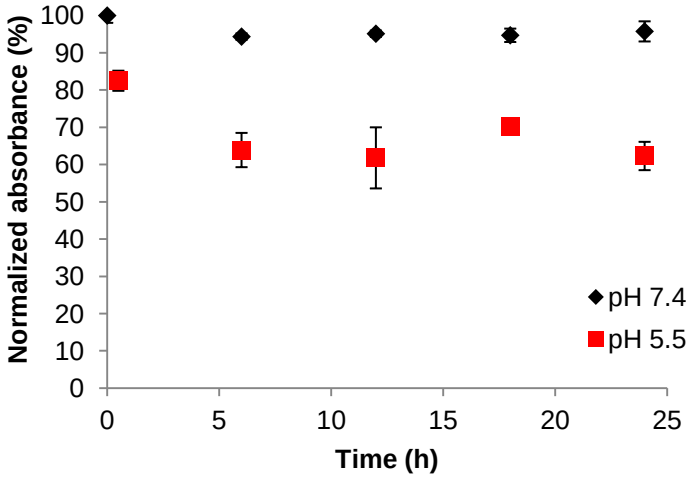

Fig. S15 The same concentration of DOX-SWCNT (with 100% drug loading) used in the degradation experiment was prepared in phosphate buffer (0.1 M, pH 7.4) and acetate buffer (0.1 M, pH 5.5) over 24 h, respectively. The free DOX released from the nanotube carrier was collected by filtration through a 10kD Amicon centrifugal filter (11,000 rpm, 10 min), and the concentration of free DOX was measured using UV-Vis at 480 nm. The error bars indicate the means ± SD of three replicate measurements.

16. MDSC abrogated cytotoxic/cytostatic effect of free DOX, but not DOX-SWCNT, on 3LL cells *in vitro*.

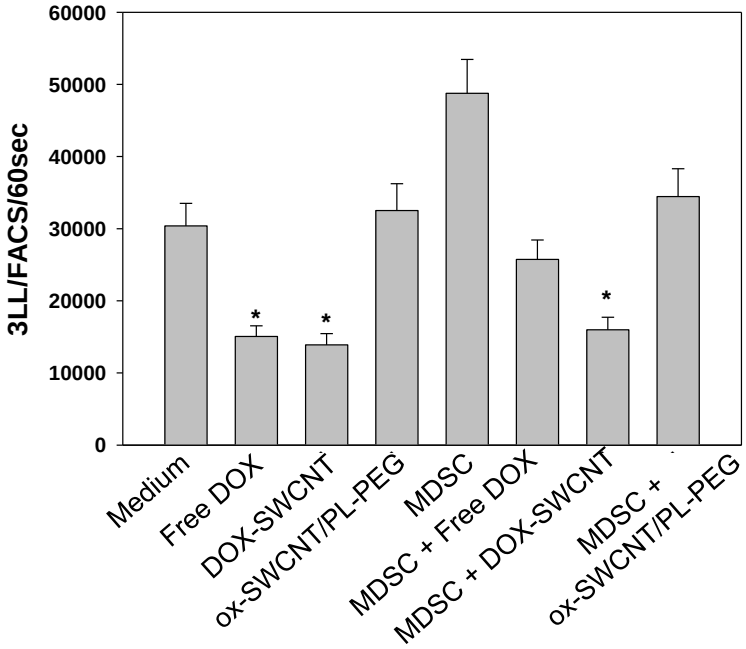

Fig. S16 3LL lung carcinoma cells and bone marrow-derived tumor-activated MDSC were generated and cultured as described in M&M. Cells were co-cultured for 24 h in the presence of soluble free DOX or DOX-SWCNT alone or together. ox-SWCNT/PL-PEG and MDSC+ ox-SWCNT/PL-PEG served as controls. The number of tumor cells was determined by assessing flow cytometry events for 60 sec as described in M&M. All cell cultures were set in triplicates and results are shown as the mean SEM (N=2). *, $p<0.01$ versus control (medium) group (One way ANOVA).

17. References

S1. J. K. Sprafke, S.D. Stranks, J.H.Warner, R.J. Nicholas and H.L. Anderson, *Angew. Chem. Int. Ed*. 2011, **50**, 2313–2316.

S2. R. V. Stevens, K. T. Chapman and H. N. Weller, *J. Org. Chem.*, 1980, **45**, 2030–2032.

S3. H. B. Dunford and L. A. Marquez-Curtis, Myeloperoxidase: Kinetic Evidence for Formation of Enzyme-Bound Chlorinating Intermediate. In Methods in Enzymology. Vol. 354; D. L. Purich. Ed. Elsevier Science: San Diego, CA, 2002; 338–350.

S4. J. Zhang, H. Zou, Q. Qing, Y. Yang, Q. Li, Z. Liu, X. Guo and Z. Du, *J. Phys. Chem. B*, 2003, **107**, 3712–3718.

S5. K. J. Reszka, M. L. McCormick and B. E. Britigan, *Biochemistry*, 2001, **40**, 15349–15361.

S6. D. M. Maniez-Devos, R. Baurain, M.Lesne and A. Trouet, *J. Pharm. Biomed. Anal*., 1986, **4**, 353–365.

S7. J. Doroshow and A. K. J. Davies, *J. Biol. Chem*., 1986, **261**, 3060–3067.

S8. D. J. Taatjes, G. Gaudiano, K. Resing and T. H. Koch, *J. Med. Chem*., 1996, **39**, 4135–4138.

S9. J. G. Sweeny, M. C. Estrada-Valdes, G. A. Iacobucci, H.Sato and S. J. Sakamura, *Agric. Food Chem*., 1981, **29**, 1189–1193.

S10. V. G. Artyukhov, O. V. Basharina, L. T. Ryazantseva and A. B. Zon, Bull. *Exp. Biol. Med*., 2001, **131**, 457–460.